5th Canadian Conf. Earthquake Engineering / Ottawa / 1987 / 5ème Conf. Canadienne Gènie Sismique

Experimental studies of friction damped braced steel frames

A.Filiatrault & S.Cherry
University of British Columbia, Vancouver, Canada

ABSTRACT: This paper presents the results obtained from qualification tests of a new friction damping system, which has been proposed in order to improve the response of Moment Resisting Frames (MRF) and Braced Moment Resisting Frames (BMRF) during severe earthquakes. The system basically consists of a special inexpensive mechanism containing friction brake lining pads introduced at the intersection of frame cross-braces. Seismic tests of a three storey Friction Damped Braced Frame model were performed on an earthquake simulator table. The experimental results are compared with the findings of an inelastic time-history dynamic analysis. The results, both analytical and experimental, clearly indicate the superior performance of the Friction Damped Braced Frame (FDBF) compared to conventional building systems.

1. INTRODUCTION

Recently a novel structural system for aseismic design of steel framed buildings has been proposed by Pall and Marsh (1). The system consists of an inexpensive mechanism containing friction brake lining pads introduced at the intersection of frame cross-braces. Fig. 1 shows the location of the friction devices in a typical steel frame. The general arrangement of an actual friction device is presented in Fig. 2.

Each brace is provided with a connection which, during a major earthquake, will slip before exceeding the yield stress of any member in the structure. Slipping of a device changes the natural frequency of the structure and the phenomenon of quasi-resonance between the structure and the earthquake excitation can be reduced. The value of the force in the brace to cause slipping must exceed the corresponding force due to wind action.

In this investigation, each friction device was provided with a compression spring which allowed adjustments to be made to the clamping force and therefore the slip load. Springs would not be used in a prototype structure; the clamping force would be developed by a bolt torqued to the proper value. Each device is provided with four friction surfaces: one friction surface in each joint and one common friction surface between the joints in the form of a washer, to which brake lining pads are attached on each side. A view of the different friction surfaces is shown in Fig. 3.

2. OPERATION OF THE FRICTION DAMPING SYSTEM

If the diagonal braces of an ordinary braced frame structure were designed not to buckle in compression, a simple friction joint could be inserted in each diagonal. In this case each slip joint would act independently of the other. However, it is frequently not economical to design the braces in compression and, more often, since the braces are quite slender, they are designed to be effective in tension only. In such cases, a simple friction joint would slip in tension but would not slip back during reversal of the tension load or in the compression (buckled) regime. The energy absorption would be relatively poor since the brace would not slip again until it was stretched beyond the previous elongated length.

The braces can be made to slip both in tension and compression simultaneously by connecting the friction mechanism shown in Fig. 2 at the intersection of frame

cross-braces. When a seismic lateral load is induced in the frame, one of the braces goes into tension while the other brace buckles very early in compression. The joint slip load should be lower than the yield load of the braces, so that the joint can be activated before the member yields. When the load in the tension brace reaches the slip load, it forces the joint to slip and activates the four links. This, in turn, forces the joint in the other brace to slip simultaneously. In this manner, energy is dissipated in both braces in each half cycle. Moreover, in each half cycle, the mechanism straightens the buckled brace and makes it ready to absorb energy immediately.

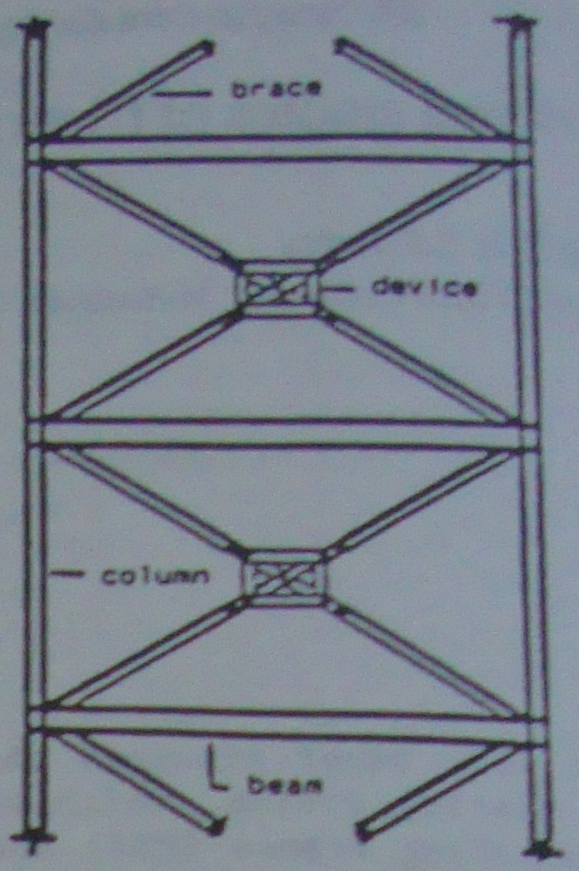

Figure 1. Location of Friction Device.

3. CALIBRATION AND QUALITY CONTROL OF FRICTION DEVICES

To be effective the friction devices must present very stable, non-deteriorating hysteresis loops. Cyclic load tests on the friction devices were carried out in a standard testing machine (2). One end of a diagonal link of the friction device was bolted to a rigid testing bench while the opposite end was attached to a vertical hydraulic actuator.

The fabrication tolerances of the friction devices were specified according to the CSA standard CAN3-S16.1-M78. The nominal diameter of the holes were drilled 2 mm greater than the nominal bolt sizes. This fabrication tolerance was found to be too large and, as a result, a rectangular hysteresis loop was not obtained. This is due to the fact that, when the loaded link slips, the 4 corner bolts of the mechanism (see Fig. 2) first slide in their holes without developing any bearing resistance. During this interval, the mechanism is not activated and energy is not absorbed in the friction joint of the other link. The problem occurs in both tension and compression.

The results of these tests clearly indicate that a rectangular load-deformation curve can only be obtained if the fabrication tolerances of the friction devices are minimized. This was achieved by inserting steel bushings in the 4 corner holes of the mechanism. As a result, the fabrication tolerance was reduced from 2 mm to 0.25 mm.

A typical hysteresis loop developed with these modified devices is shown in Fig. 4. The hysteresis loop is very nearly a perfect rectangle and exhibits negligible fade even after 50 cycles.

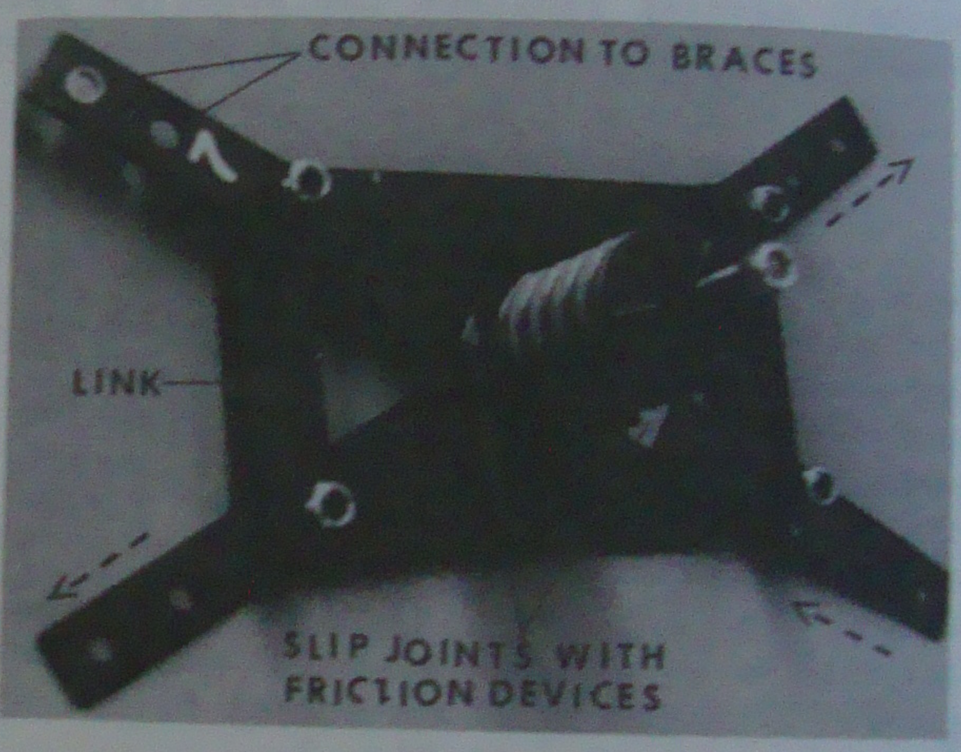

Figure 2. Friction Device.

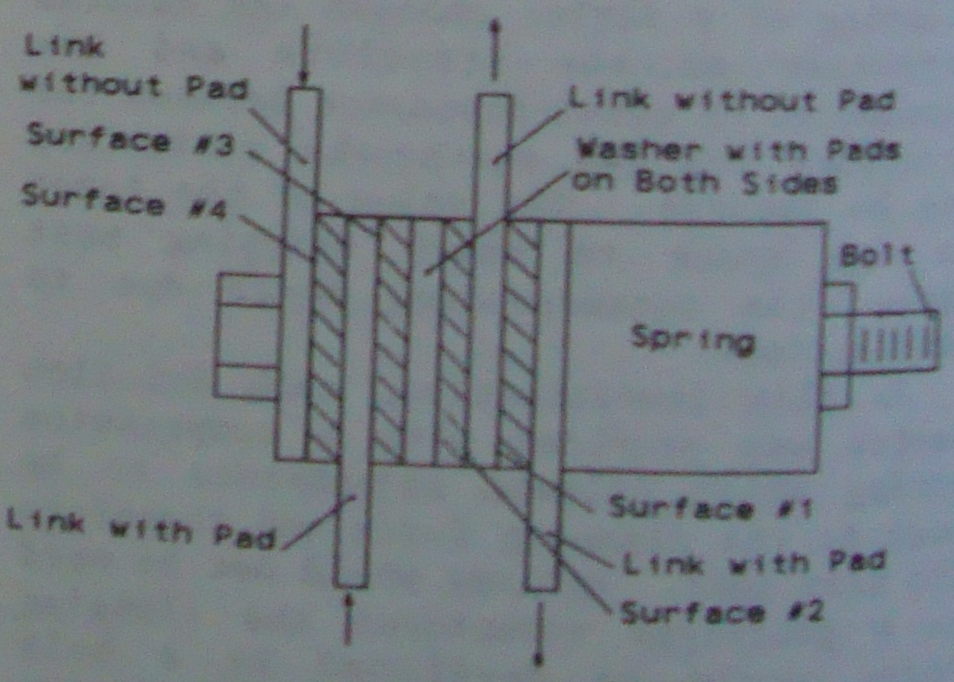

Figure 3. Friction Surfaces of Friction Device.

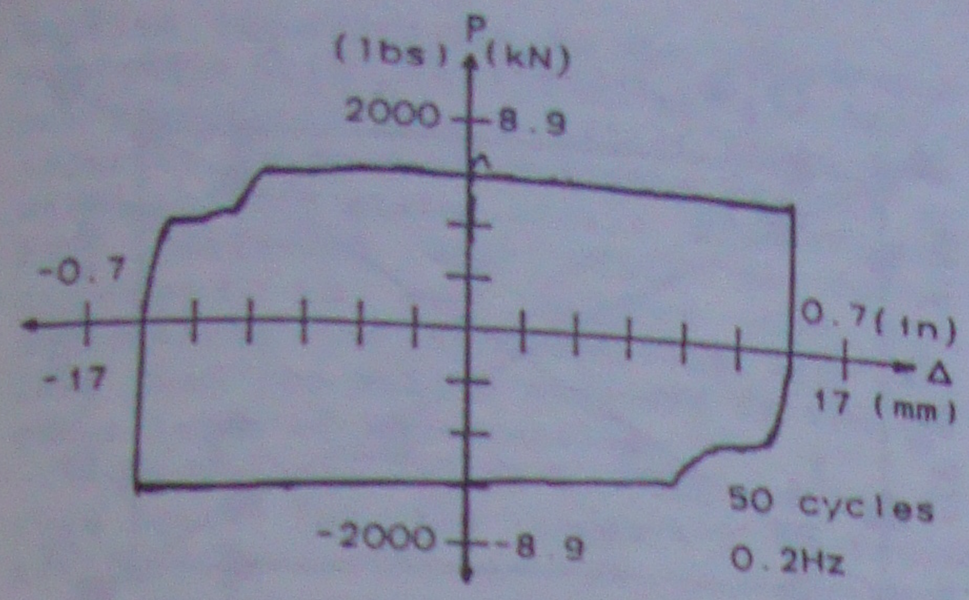

Figure 4. Hysteresis Loop From Friction Device.

In order to calibrate the friction devices, seven devices were tested under repeated cyclic loads with different values of the spring load. Before each test, the length of the compression spring was measured with a precision vernier. It was then possible to establish a correlation between the slip load and the length of the compression spring. For each device a linear regression analysis was performed to obtain an equation relating the global slip load and the spring length. The resulting equations represent calibration curves for the friction devices. These curves are plotted with the experimental data in Fig. 5.

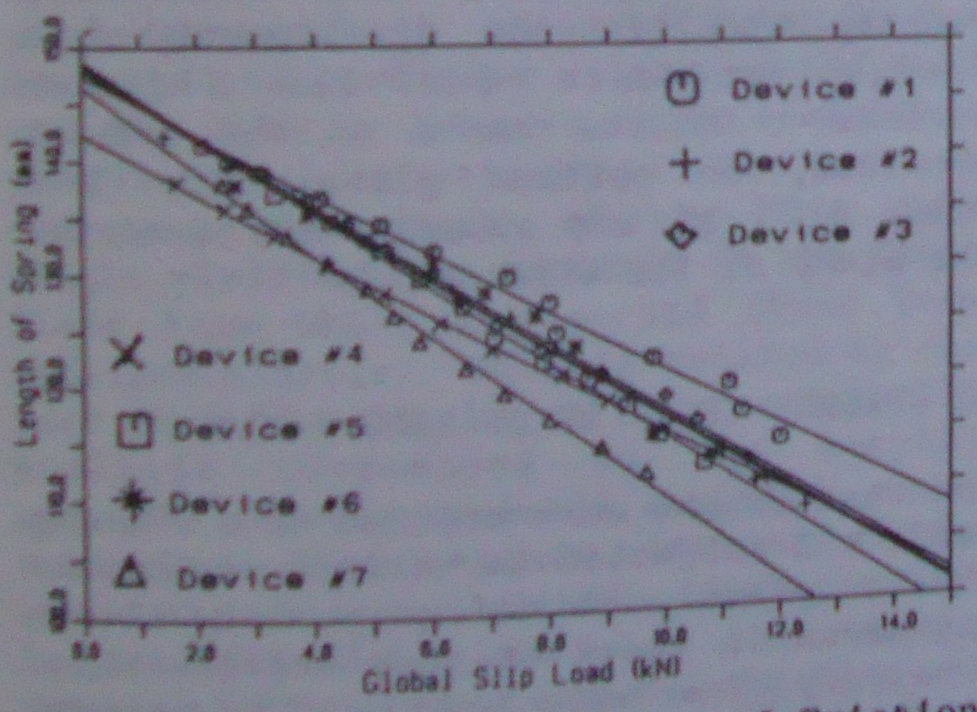

Figure 5. Calibration Curves of Friction Devices.

4. DESCRIPTION OF TEST FRAMES

A 1/3 scale model of a 3 storey FDBF was used in the shake table tests (2). The overall dimensions of the model frame were 2.05×1.40 m in plan and 3.53 m in height. All the main beams and columns were made of the smallest shapes (S75×8) available. The dead load was simulated by concrete blocks at each floor. The dead load of each concrete block was transmitted to its supporting beams through the flanges of 6 channels welded to these main members. With this system, representing point loading, the diaphragm effect of the concrete was reduced. Two identical frames were fabricated for the experimental study. The beam-column connections were designed such that the FDBF could be transformed easily into an MRF or a BMRF as needed. The general arrangement of the test frame is shown in Fig. 6.

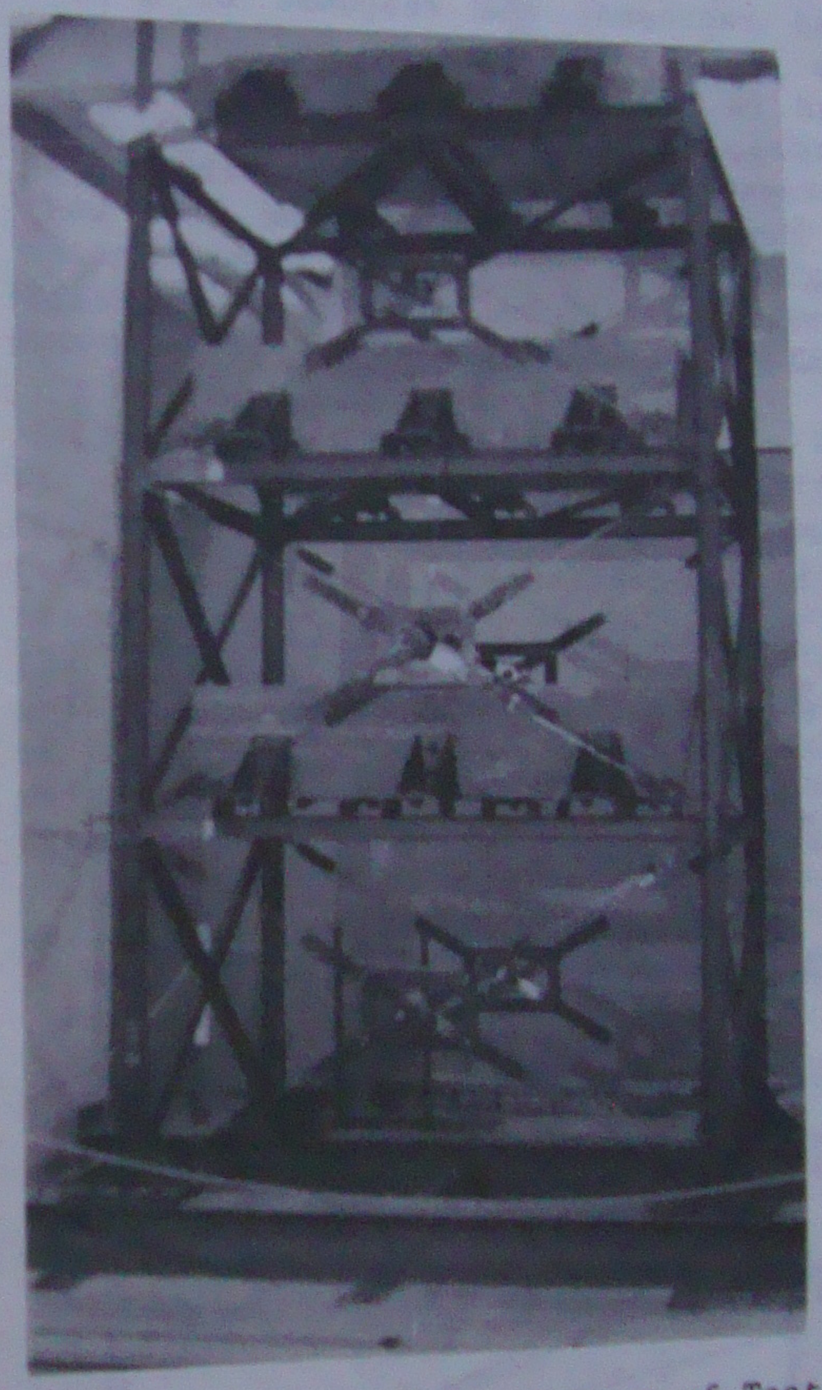

Figure 6. General Arrangement of Test Frame

5. OPTIMUM SLIP LOAD STUDY

The energy dissipation of a friction device is equal to the product of slip load by the total slip travel. The optimum slip load is the load which leads to maximum energy dissipation in the friction device. To determine the optimum slip load of the model frame, inelastic time-history dynamic analyses were performed for different values of the

slip load using the computer program "DRAIN-2D".

The optimum slip load study was carried out for 3 different earthquake records: El Centro 1940 N-S and Parkfield 1966 N65E, both scaled to 0.52 g; Newmark-Blume-Kapur artificial accelerogram scaled to 0.3 g. Typical results of the optimum slip load study are given in Fig. 7, which shows envelopes of lateral deflections for global slip loads ranging from 0 to 10 kN, representing the elastic region of the cross-braces. Similar curves were obtained for response envelopes of beam and column moments and shears. Results for zero global slip load represent the response of a MRF. The global slip load is defined as the load in the tension brace when slippage occurs, while the local slip load represents the load in each friction pad at the same time. From the free body diagram shown in Fig. 8, the relation between the global slip load and the local slip load is given by:

$$P_g = 2P_\ell - P_{cr} \qquad (1)$$

where P_{cr} is the critical buckling load of the compression brace.

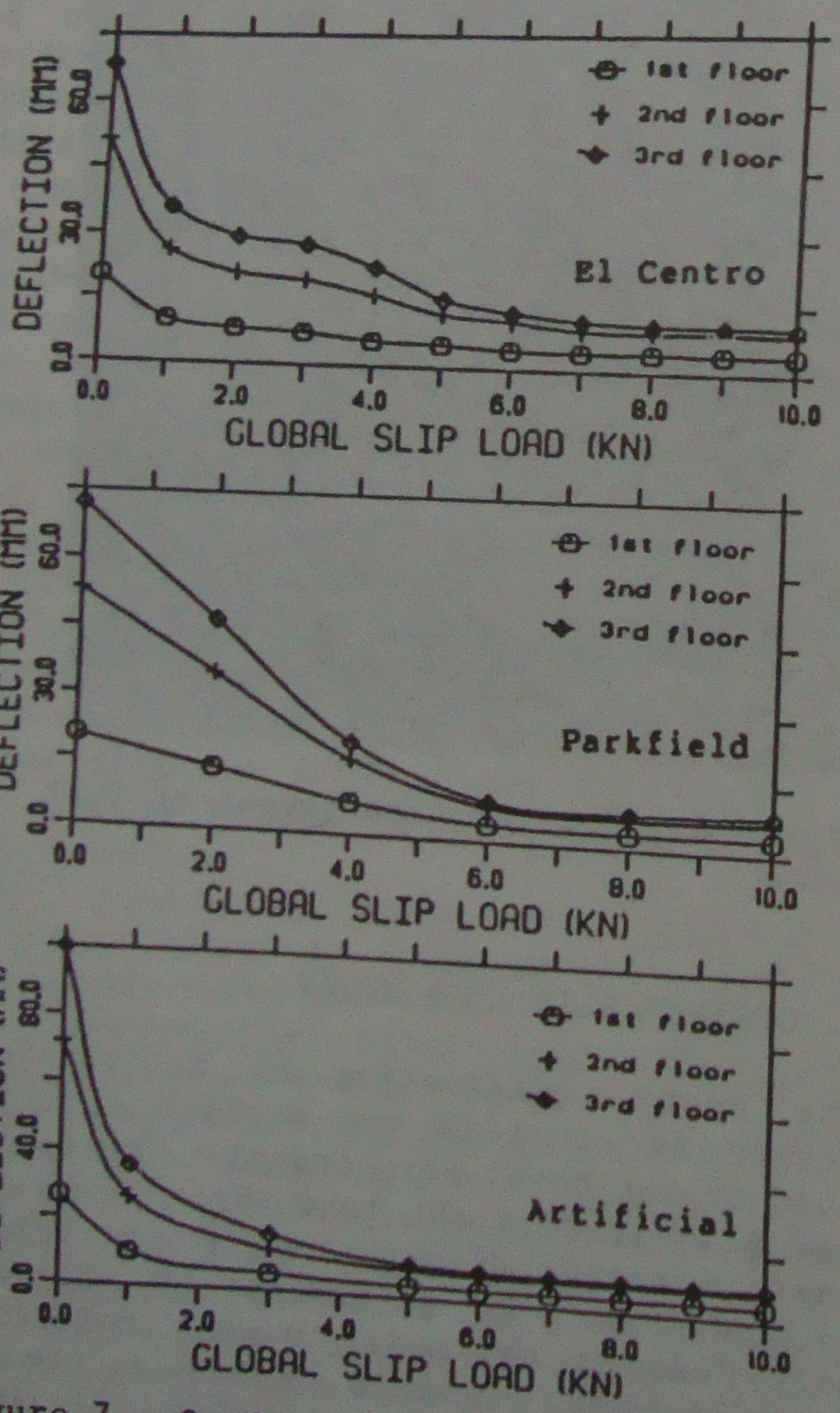

Figure 7. Optimum Slip Load Study (Envelopes of Lateral Deflections)

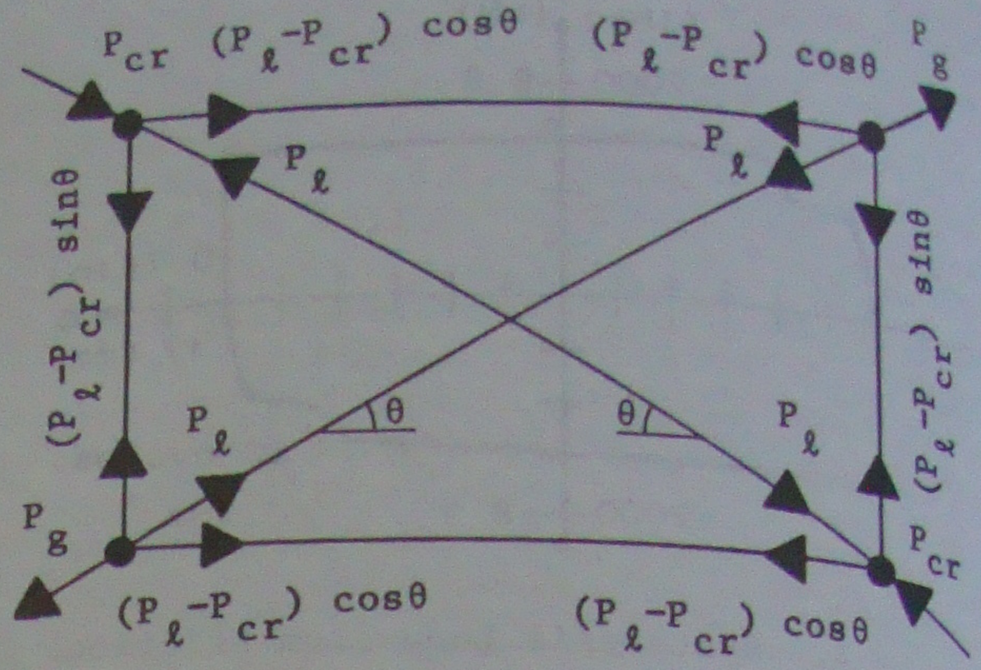

Figure 8. Free Body Diagram of a Friction Device at Slipping.

Figure 7 clearly shows the effectiveness of the friction devices in improving the seismic response of the frame. As the global slip load is increased, the deflections decrease steadily up to a global slip load of 6 kN. For a global slip load between 6 kN and 10 kN, there is very little variation in the response. This lower bound value of 6 kN for the global slip load is observed for the 3 different earthquakes studied. This suggests that the optimum value of the global slip load may be independent of the ground motion input. If this is found to hold true for all cases, the optimum slip load can be considered as a structural property. A more general verification of this observation may greatly simplify the development of a design procedure for the friction devices. On the basis of the results obtained, an optimum global slip load value of 7 kN was subsequently used for the study of the FDBF model.

6. SEISMIC TESTS ON SHAKING TABLE

The test frames were mounted on a shaking table and subjected to various earthquake accelerograms with different intensities expressed in terms of peak acceleration. A variety of sensors were used to measure displacement, acceleration, friction pad slippage and strain at critical locations in the frame.

The MRF and BMRF did not perform well during the tests corresponding to a major earthquake. Very large strains occurred in the base column, and in the first and second floor beams of the MRF. Although the main structural members of the BMRF remained elastic, many cross-braces yielded in tension. The elongation of the braces was very large and they

buckled significantly in the compression regime; this indicates that heavy non-structural damage likely would have occurred in a real building (cracks in walls, broken glass, etc.). However, the FDBF performed very well; no damage occurred in any member and the deflections and accelerations were far less than the values measured in the two other types of construction.

The envelopes of the bending moments in the beams for the Newmark-Blume-Kapur artificial earthquake at 0.3 g peak acceleration are presented in Fig. 9.

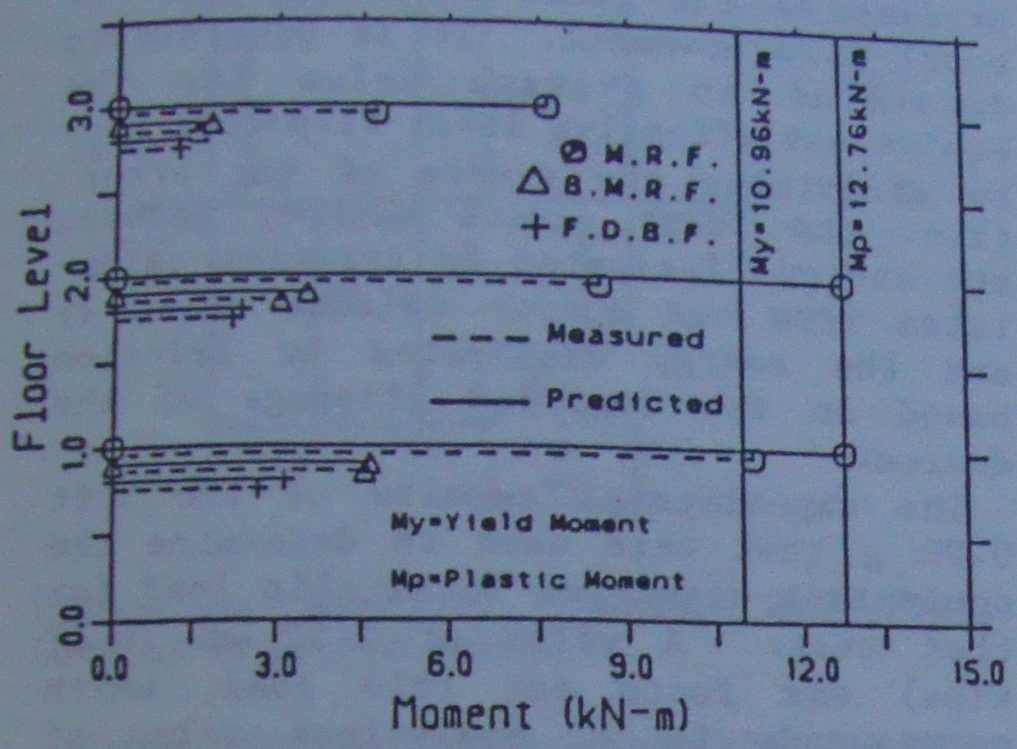

Figure 9. Envelope of Bending Moments in Beams (Artificial 0.30 g).

The effectiveness of the friction devices in improving the seismic response of the frames is clearly shown. Also, good agreement is observed between the measured and predicted values of the BMRF and the FDBF. However, the analytical prediction overestimates the actual damage in the beams of the MRF; only slight yielding was measured in the first floor beam while the second floor beam remained elastic. This is related to the fact that the damping values used in the analysis correspond to the damping measured under very small amplitude excitations. These values are not representative of the actual damping under large amplitude vibrations; the damping values of the model frames would increase with the amplitude of motion. The use of larger damping values in the analysis would reduce the difference between the predicted and measured values for the MRF.

Figure 10 shows the measured and predicted slippage time-histories for the second floor device during the first 9 seconds of the 0.3 g Artificial earthquake. Considering the noisy signal recorded, the agreement between the measured slippage, and the corresponding values predicted by using the analytical model, is reasonable.

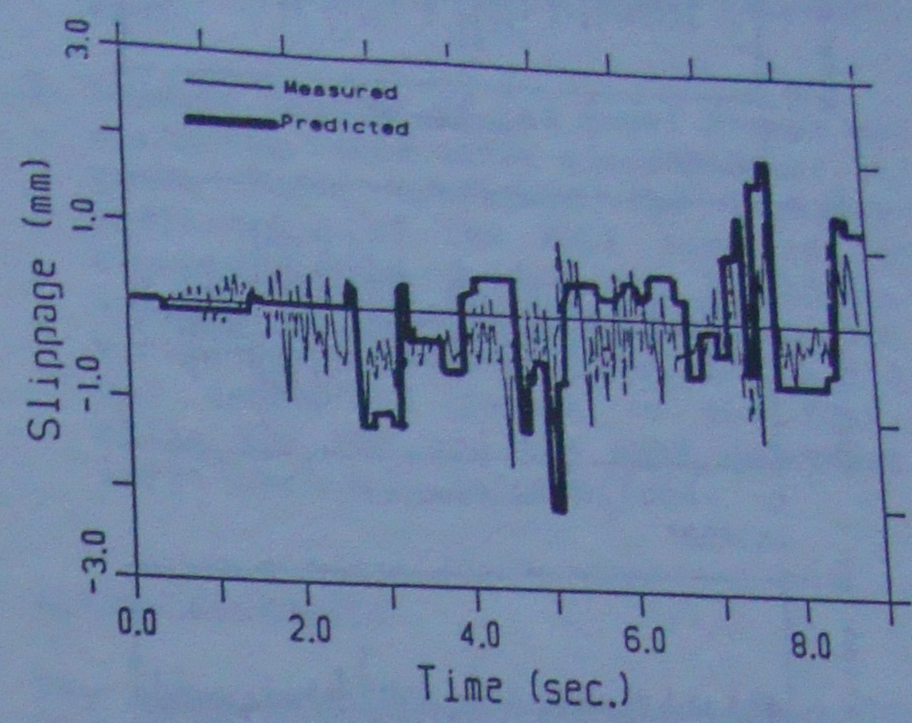

Figure 10. Slippage Time-Histories of Second Floor Device (Artificial 0.30 g).

The torsional motion developed in the structure was determined by calculating the difference between the displacement records given by the parallel plane frames at each floor. Figure 11 shows the time-history of the third floor deflection recorded on each plane frame of the FDBF during the 0.3 g Artificial earthquake. The two signals are in phase with almost equal amplitudes and therefore no significant torsional stresses were induced in the structure.

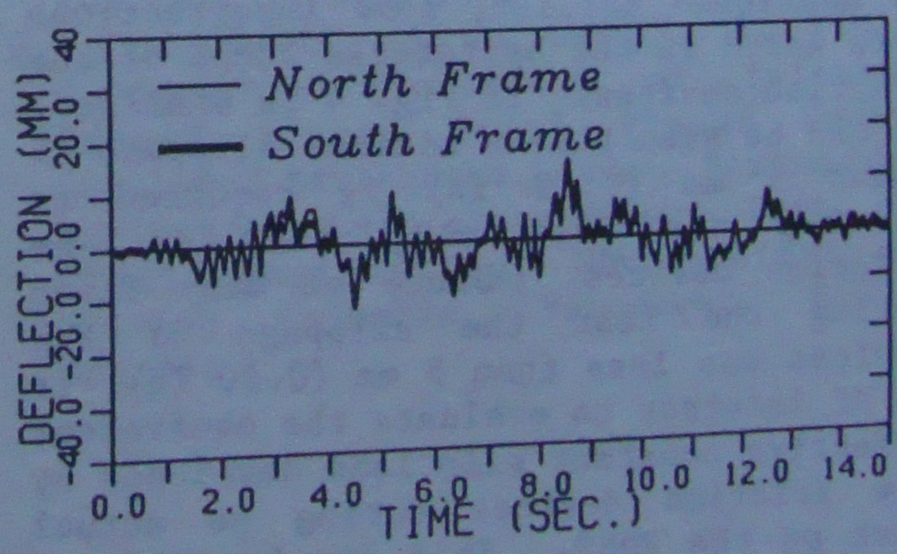

Figure 11. Third Floor Deflection of Each Plane Frame (Artificial 0.30 g).

Figure 12 shows typical response characteristics of the three structural configurations expressed in terms of the measured horizontal accelerations when subjected to an extremely severe earthquake: Taft 1952 scaled to a peak acceleration of 0.9 g.

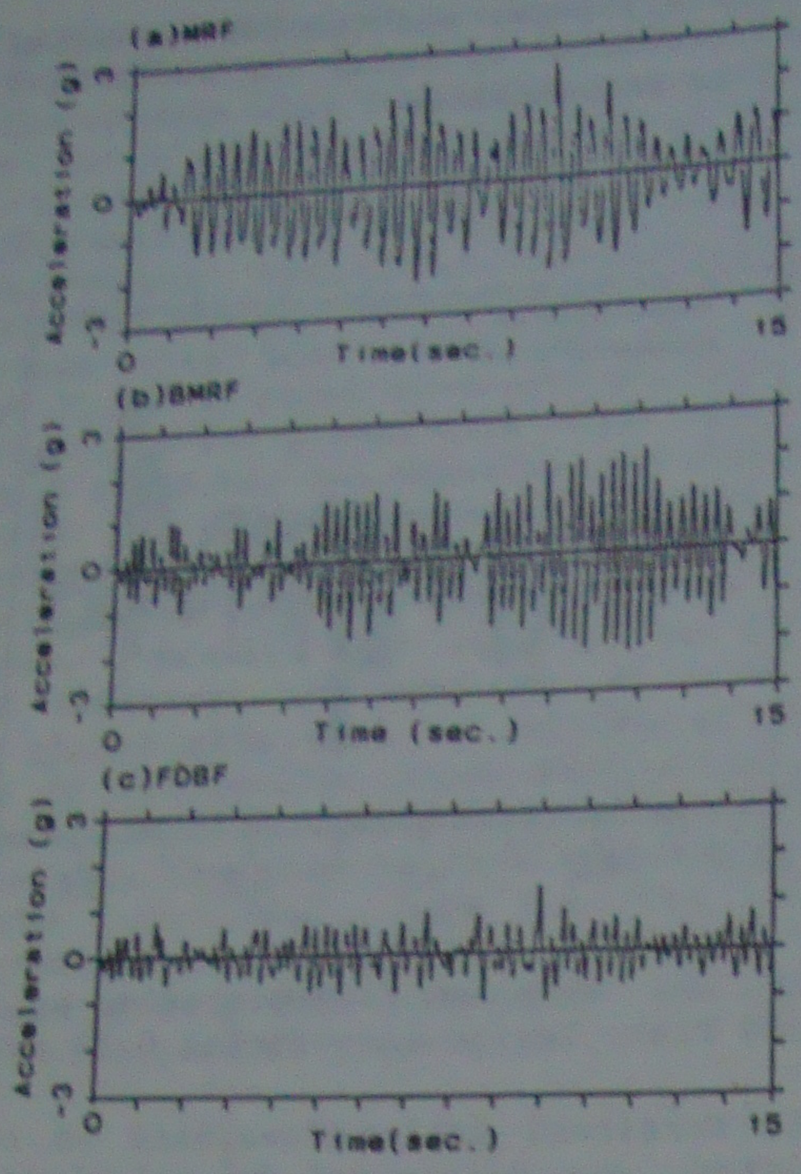

Figure 12. Measured Third Floor Accelerations (Taft 0.90 g).

A peak acceleration of 1.42 g was measured at the top of the FDBF compared to peak acceleration values of 2.24 g and 2.67 g for the BMRF and the MRF respectively.

7. ENERGY BALANCE

As mentioned earlier, some imperfections were noted in the hysteresis loops of the friction devices. If Fig. 4 is examined, it can be seen that a minimum slippage of about 5 mm (0.20 in) is required to develop the full slip load of the friction devices. Since at many times during the test the slippage of the devices was less than 5 mm (0.20 in), it is of interest to evaluate the equivalent effective constant slip load developed by the friction devices during an actual test on the FDBF. This can be achieved by considering an energy balance of the system.

At any instant of time the energy balance equation is expressed as:

$$E_F = E_{in} - V - T - L \qquad (2)$$

where

E_{in} = Energy input to the structure,
V = Potential Energy | Energy Stored,
T = Kinetic Energy
L = Energy dissipated by viscous damping,
E_F = Energy dissipated by friction.

All the terms on the right hand side of Eqn. (2) can be evaluated using the recorded data from an actual test on the shaking table. The energy input to the structure is the product of the base shear and table displacement. The energy dissipated by friction is equal to the product of the local slip load and the total slip movement. It is possible to determine an average value for the equivalent effective local slip load (P_ℓ) by minimizing the square of the error (i.e. the least square method) between the energy dissipated by friction calculated from the energy balance (Eqn. 2) and the energy dissipated by friction based on the recorded slippage of the device.

The experimental results of the Taft 0.90 g test were used to determine the equivalent effective local slip load for that test. A value of 2.52 kN (0.57 kips) was found for this load, which corresponds to an equivalent value of only 5.04 kN (1.13 kips) for the global slip load instead of the calibrated value of 7 kN (1.57 kips) which was initially set on the devices. The resulting time-history plots of the energy inputs, the energy absorbed by the friction devices and the energy dissipated by viscous damping are presented in Fig. 13.

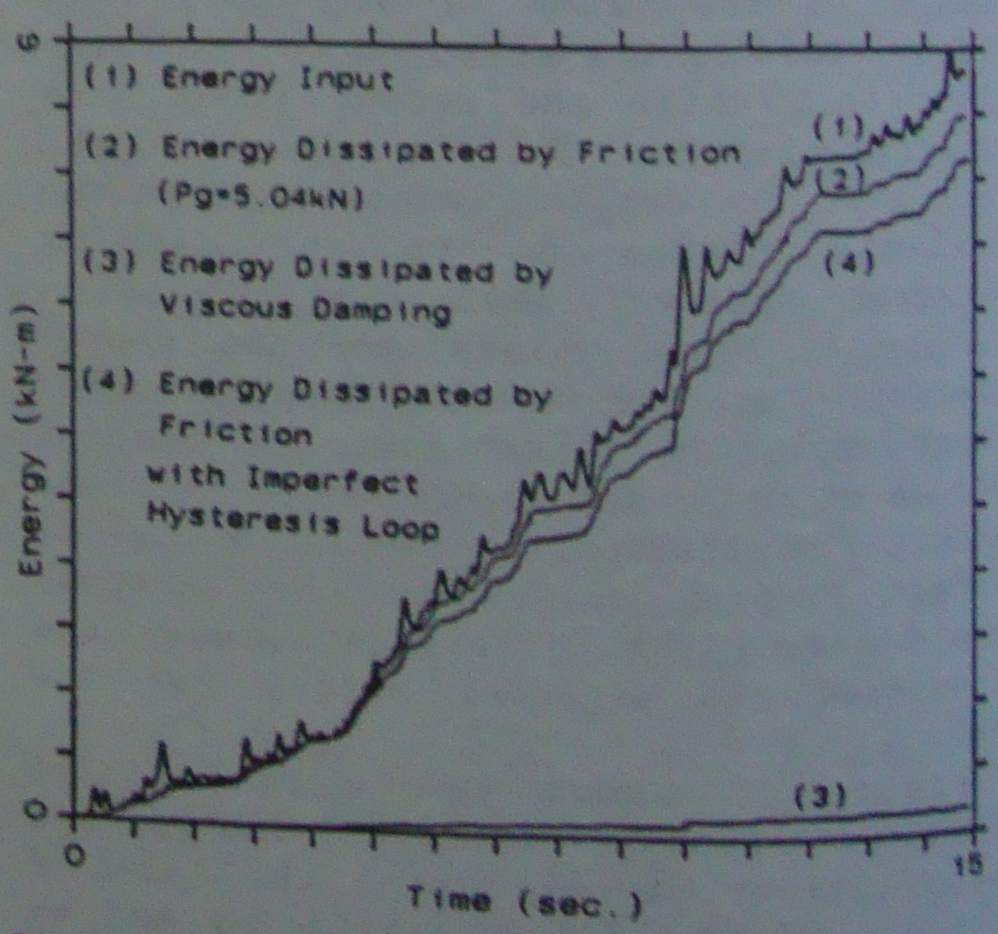

Figure 13. Energy Balance (Taft 0.90 g).

Figure 13 also shows a curve of the energy dissipated by friction using an idealized model, Fig. 14, of the experimentally measured imperfect hysteresis loops (see Fig. 4). For this calculation, all the friction devices were represented by this average model. It can be seen that the two curves showing energy dissipated by friction agree reasonably well.

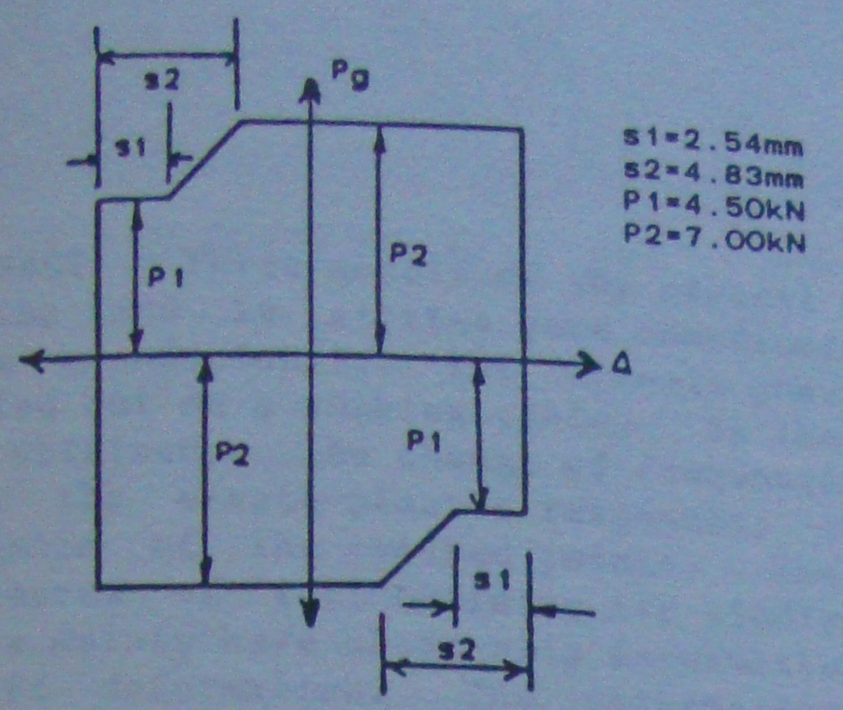

Figure 14. Model of Imperfect Hysteresis Loop of Friction Devices.

These results confirm that the friction devices were not acting at the optimum slip load of the structure, apparently due to the fact that the fabrication tolerance was still too large. In order to be fully effective, the friction devices should be fabricated in a precision shop with minimum construction tolerance. However, even though the optimum slip load was not obtained, the structural response of the FDBF was demonstrably superior to the responses of the two other types of frame construction.

8. CONCLUSIONS

1. The friction devices were first tested under cyclic loads in order to study the stability of the brake lining pads and to calibrate their slipping loads. The results of the experiments clearly indicate that the behaviour of the pads is very stable even after 50 cycles. It is likely that the devices will produce a rectangular hysteresis loop if the fabrication tolerances of the friction devices are minimized.

2. An analytical study was performed to determine the value of the slip load which optimized the energy dissipation of the friction devices. The results seem to indicate that the optimum slip load may be independent of the ground motion time-history and is rather a structural property. Further studies are needed to confirm this observation.

3. Seismic testing of the model frames on a shaking table under simulated earthquake loads confirmed the superior performance of the FDBF compared to conventional aseismic building systems. Even an earthquake record with a peak acceleration of 0.90 g did not cause any damage to the FDBF, while the MRF and the BMRF underwent large inelastic deformations.

ACKNOWLEDGEMENTS

The work reported was carried out under Contract No. 1ST84-00045 with the Department of Supplies and Services, Canada; the scientific authority for this contract was assigned to the Division of Building Research, National Research Council of Canada. The authors acknowledge the fruitful discussions which were held with Dr. A.S. Pall, and the help of the Canadian Institute of Steel Construction.

REFERENCES

1. PALL, A.S. & MARSH, C. 1982. Response of Friction Damped Braced Frames. ASCE, Journal of Structural Division, Vol. 108, ST6: 1313-1323.
2. FILIATRAULT, A. & CHERRY, S. 1985. Performance Evaluation of Friction Damped Braced Steel Frames Under Simulated Earthquake Loads. Earthquake Engineering Laboratory Report, Dept. of Civil Engineering, University of British Columbia, Vancouver, B.C., Canada.